Simple and Modestly Scalable Synthesis of *iso*-Cyrene from Levoglucosenone and Its Comparison to the Bio-Based and Polar Aprotic Solvent Cyrene®

Xin Liu,[a,†] Brett Pollard, [a,†] Martin G. Banwell,[a,b,*] Li-Juan Yu,[a] Michelle L. Coote,[a] Michael G. Gardiner,[a] Barbara M. A. van Vugt-Lussenburg,[c] Bart van der Burg,[c] Fabien L. Grasset,[d] Elisabeth Campillo,[d] James Sherwood,[e] Fergal Byrne[e] and Thomas J. Farmer[e]

† These authors contributed equally to the work

[a] Research School of Chemistry, Institute of Advanced Studies, The Australian National University, Canberra, ACT 2601, Australia.
[b] Institute for Advanced and Applied Chemical Synthesis, Jinan University, Guangzhou, 510632, China.
[c] BioDetection Systems bv, Science Park 406, 1098XH Amsterdam, The Netherlands
[d] V. Mane Fils, 620 route de Grasse, 06620 Le-Bar-sur-Loup, France
[e] Green Chemistry Centre of Excellence, Department of Chemistry, University of York, Heslington, York, YO10 5DD, UK.

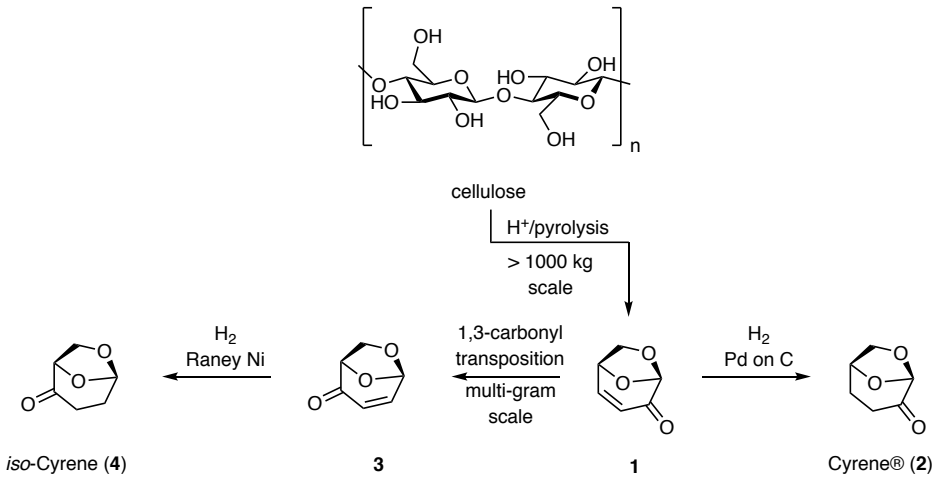

ABSTRACT: The bio-derived platform molecule levoglucosenone (LGO, **1**), which is the precursor to the green solvent Cyrene® (**2**), has been converted, at multi-gram scale, into its pseudo-enantiomer (*iso*-LGO, **2**) and this reduced to *iso*-Cyrene (**4**). A less effective synthesis of this last compound from *D*-glucose is also described. Various physicochemical as well as certain toxicological properties of compound **4** are reported and compared to those established for the now commercially available Cyrene® (**2**). Such studies reveal that there are significant enough differences in the properties of the sustainably-derived Cyrene® (**2**) and isomer **4** (*iso*-Cyrene) to suggest they will exert complementary effects as solvents in a range of settings.

Key Words: bio-derived, Cyrene®, green solvent, *iso*-Cyrene, levoglucosenone

Introduction

Organic solvents represent a major proportion of the chemicals currently derived from the petroleum industry. In order to achieve more sustainable manufacturing regimes, there is an increasing interest in identifying and establishing routes to bio-derived solvents.[1] Arguably, the most recent and notable development in this area has been the high-volume, pyrolytic conversion of acid-treated cellulose into the small molecule levoglucosenone (**1**) (Figure 1) and the reduction of this into its dihydro-derivative **2**.[2-4] The latter compound is now marketed as Cyrene®,[5] a bio-derived solvent that displays a range of useful properties and such that it is touted as a replacement for the widely-deployed and petroleum-derived *N*-methylpyrrolidine (NMP). This is because, inter alia, NMP displays reproductive toxicity[2] while Cyrene® has tested negative for such properties as well as mutagenicities and is, additionally, almost completely non-ecotoxic (LD_{50} >2000 mg/L).[6]

Our ongoing interest in exploring and expanding the chemical utility of LGO (**1**),[7,8] which can now be regarded as an abundant fine chemical, promoted us to refine our earlier route from this compound to its pseudo-enantiomer *iso*-LGO (**3**) so as to produce the latter compound on a multi-gram scale and then reduce this to form *iso*-Cyrene (**4**). Such an outcome would allow for the evaluation of the solvent properties of ketone **4**, a compound that has received little attention experimentally. Indeed, it only appears to have been prepared on two previous occasions,[9,10] the first being in the 1970s[9a] and whereby a β,D-*arabino*-hexopyranose derivative was converted into compound **4** over multiple steps. The second synthesis was reported[10] in 2018 and involved the reduction of *iso*-LGO (**3**) that had been generated by a protocol closely related to the one we described[8] in 2018. In each case *iso*-Cyrene was obtained in sub-gram quantities.

While, in various respects, the solvent properties of Cyrene® and *iso*-Cyrene are expected to be similar,[3] the pseudo-enantiomeric relationship between them might ultimately be the most significant difference by allowing their complementary use in facilitating/enhancing enantioselection in certain organic transformations or in the fractional crystallization (resolution) of racemic compounds. In a related vein, it could also serve as a chiral auxiliary and (perhaps) act in a complementary fashion to Cyrene®.[11] The presence of the internal and inductively electron-withdrawing acetal residue adjacent to the ketone carbonyl within

Cyrene® as well as possibilities for intramolecular hydrogen bonding[9a] creates a capacity to form the corresponding hydrate,[9a,12] a feature that has been used to "tune" its solvent properties.[12] Given the more remote relationship between the equivalent residues within *iso*-Cyrene (**4**) then hydrate formation should be a less significant process in this case,[9] a feature that may prove advantageous in some instances. Such considerations provided the motivation for the study detailed herein.

Figure 1: The structures of the bio-derived platform molecule levoglucoseone (**1**), its dihydro-derivative Cyrene® (**2**) and their isomeric congeners **3** and **4**.

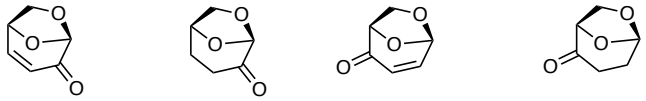

1 Cyrene® (**2**) **3** *iso*-Cyrene (**4**)

Results and Discussions

Synthetic Studies

The synthetic sequence used to accumulate *iso*-Cyrene at a 10 gram scale from LGO (**1**) is shown in Scheme 1 and was informed by our earlier studies. In particular, the necessary 1,3-carbonyl transposition still exploited the operationally simple and triethylamine-catalyzed conjugate addition of water to LGO and thereby forming the previously reported[8,13,14] hydroxyketone **5** which was obtained in 72% yield as a clear, colorless oil. The high α-face diastereoselectivity of this process is as expected and largely determined by the steric demands of the 1,6-anhydro-type bridge occupying the β-face of 2*H*-pyran-3(6*H*)-one core of the substrate. Accompanying product **5** were small amounts (0.5%) of the chromatographically separable and previously reported[15] dimeric compound **6**, the structure of which was confirmed by single crystal X-ray analysis (see the Experimental and Supporting Information – SI – for details). Compound **6** is presumed to arise through the participation of the starting enone **1** in a triethylamine-catalyzed intermolecular Rauhut-Currier or vinylogous Morita-Baylis-Hillman reaction.[16] Reductive amination of ketone **5** was accomplished using dimethylamine and hydrogen in the presence of 10% Pd on C and afforded a 1:3 mixture of the epimeric forms of amine **7**. A range of reagents was explored for the purposes of converting the hydroxyl group in this last compound into the β-aminoketone **7** but the only ef-

Scheme 1: Synthetic sequence leading from LGO (**1**) to *iso*-Cyrene (**4**).

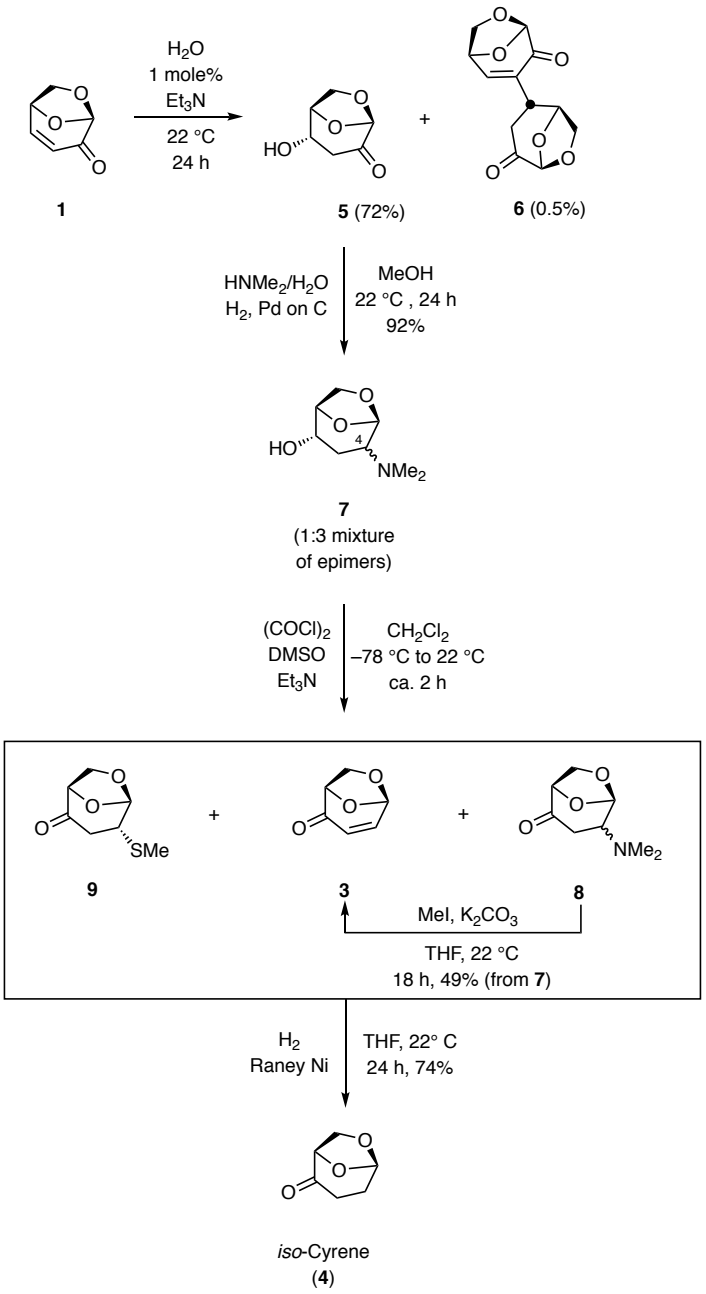

-fective oxidant, among dozens tested, proved to be the Swern reagent.[17] As a consequence, when the relevant conditions were employed then a mixture of the target ketone **7**, the oxidation/elimination product *iso*-LGO (**3**) and the sulfide **9** was obtained. We assume that the last product, which could be isolated in pure form and 13% yield by conventional chromatographic techniques, arises through initial (and diastereofacially selective) conjugate addition of dimethyl sulfide (the by-product of the Swern oxidation)[17] to *iso*-LGO (**3**) with the

resulting trialklylsulfonium ion the undergoing demethylation, perhaps through nucleophilic attack by triethylamine,[18] to give the compound **9**. The conversion of product **7** into *iso*-LGO (**3**) was achieved by treating the crude mixture from the oxidation reaction with methyl iodide and potassium carbonate in THF at ambient temperatures and so affording, after flash chromatography, the latter in 49% yield (albeit still containing traces of sulfide **9**). The conversion of *iso*-LGO into its dihydro-congener was first attempted by using the same conditions as employed in the conversion **1** → **2**,[14] *viz*. by using hydrogen in the presence 10% Pd on C. However, this reduction proved sluggish at ambient temperatures with complete conversion requiring many days. This situation may be attributed to catalyst poisoning by sulfur residues present in the substrate. In contrast, when Raney nickel (W2) was employed in the presence of hydrogen at 22 °C then *iso*-Cyrene was obtained in 74% yield after 24 h. GC/MS analysis of this material indicated that it still contained *ca*. 5% of compound **9** and this is despite the capacity of Raney nickel to effect desulfurization reactions.

In order to accumulate the ca. 10 gram sample of *iso*-Cyrene (**4**) deemed necessary for a meaningful evaluation of its physical and biological properties, it was most convenient to repeat the reaction sequence shown above (and detailed in the Experimental) multiple times. This approach highlights the most obviously restrictive feature associated with the approach, namely the need to apply Swern oxidation conditions to amino-alcohol **7** and thus affording a mixture of amino-ketone **8**, *iso*-LGO (**3**) and sulfide **9**.

Given the difficulties just described, we also examined the route from *D*-glucose (**10**) to *iso*-LGO (**3**) reported by Horton and co-workers in 1996[19] (Scheme 2). In this approach the starting hexose **10** was converted into the bis-acetonide **11** (74%) with the most effective catalyst system for this purpose being a combination of H_3PO_4 and $ZnCl_2$ – using either sulfuric acid or this in combination with $CuSO_4$ led to the co-production of tar-like by-products. The structure of compound **11** was confirmed by single-crystal X-ray analysis (see Experimental and SI for details) and the associated free 2°-alcohol was esterified using *p*-toluenesulfonyl chloride in pyridine to afford the crystalline sulfonate **12** (83%) and the structure of this also confirmed by single-crystal X-ray analysis (See Experimental and SI for details).[20] Reaction of ester **12** with potassium *tert*-butoxide in THF at 0 °C for 2 h effected

the anticipated elimination reaction in a regio-selective manner to afford the dihydrofuran **13** albeit in quite variable yield because it sometimes proved difficult to drive the reaction to completion and, exacerbating matters, to separate the product from the starting material. Treatment of enol ether **13** with $AlCl_3$ under the rather specific conditions defined by Horton[19] resulted in cleavage of the associated acetonide residues and thereby affording *iso*-LGO (**3**) albeit in highly variable and normally low yield (*ca*. 30% at best in our hands). A plausible mechanistic pathway for this last (and crucial) step has been proposed by Horton.[19] All the spectral data acquired on the samples of compound **3** prepared by this route matched those reported[19] as well as those derived from the material generated using the protocols shown in Scheme 1. Raney-nickel catalyzed hydrogenation of *iso*-LGO (**3**) generated by the route shown in Scheme 2 proceeded as before and thus affording *iso*-Cyrene (**4**) in 74% yield.

Scheme 2: The synthesis of *iso*-Cyrene (**4**) from *D*-glucose (**10**)

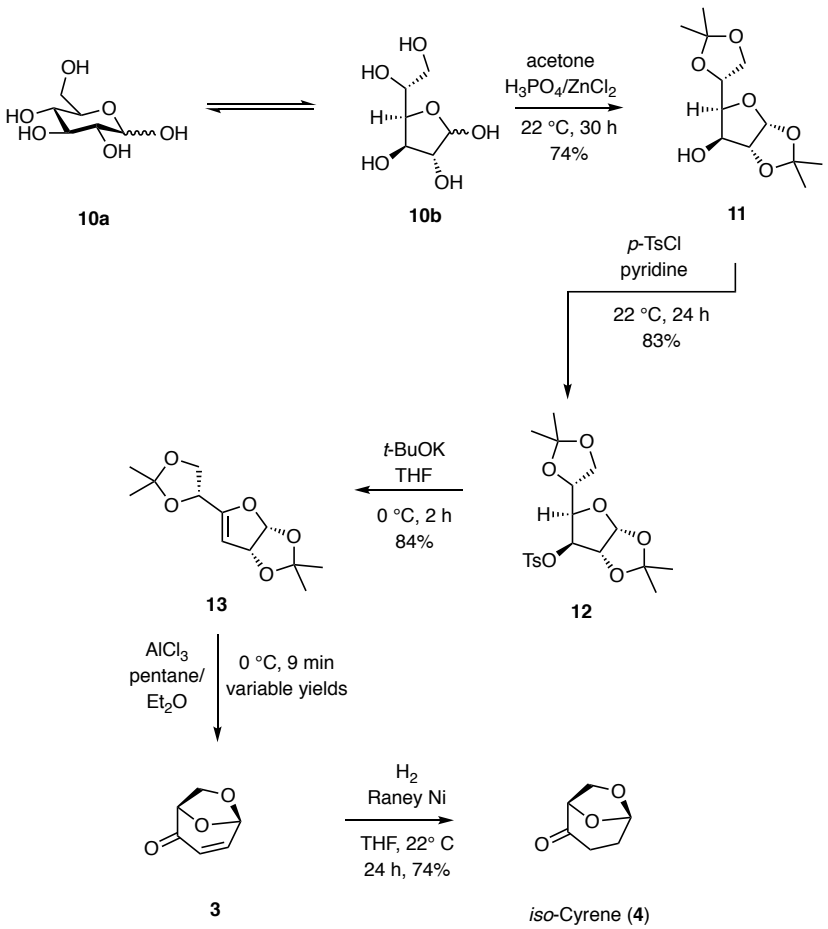

While the samples of compound **4** produced by this second route were uncontaminated by thio-ether **9**, the reaction sequence was less attractive than the first in a number of respects. In particular, it lacked many of the atom-economical features of the first route, it was operationally more tedious to prosecute and the third and fourth steps, viz. the sequence **12** → **13** → **3**, proved capricious and low-yielding, at least in our hands. On balance, then, at the present time we favor the route shown in Scheme 1 for the purposes of generating serviceable quantities of *iso*-LGO (**3**) and, thence, *iso*-Cyrene (**4**). The multi-gram accumulation of *iso*-Cyrene (**4**) by the route shown in Scheme 1 allowed for evaluations of various of its spectroscopic, physical, chemical and biological properties. Details are presented in the following sections.

Spectroscopic Studies

A comparison of the ^{1}H NMR spectroscopic data recorded on Cyrene® (**2**) with those acquired for *iso*-Cyrene (**4**) is provided in Table 1. This reveals that the dioxymethine proton associated with the former compound resonates at significantly higher field (δ_H 5.01) than its counterpart (δ_H 5.73) in isomer **4**. This difference can be attributed to the acetal proton of the former compound sitting within the shielding zone of the adjacent ketone carbonyl residue and so serving to emphasize the proximity and, therefore, the interactions between these two residues. The chemical shift differences between the resonances due to the remaining protons are much less pronounced.

Table 1: The ^{1}H NMR spectral data recorded for compounds **2** and **4**[a]

Compound	**δ_H, proton count, multiplicity, couplings**						
Cyrene® (**2**)	5.01, 1H s	4.64, 1H s	3.98, 1H d *J* 7.7[b]	3.88, 1H m	2.58, 1H m	2.35-2.16 2H, cm[c]	1.96 1H m
iso-Cyrene (**4**)	5.73, 1H, broad s	4.50, 1H, d, *J* 5.6	3.97, 1H, d, *J* 8.0	3.87, 1H, dd *J* 8.0, 6.0	2.47, 2H *J* 7.6	2.21-2.11 1H, cm[c]	2.04 1H m

[a] Spectra recorded in $CDCl_3$ at 400 MHz; [b]coupling constants presented in Hz; [c] cm = complex multiplet

An analogous comparison of the chemical shifts of the resonances due to the constituent carbons observed in the ^{13}C NMR spectrum of compound **4** with those recorded for congeners

1-**3** is presented in Table 2 and reveals that it (*iso*-Cyrene) shows the most deshielded signal for the associated ketone carbonyl resonance.

Table 2: The ^{13}C NMR chemical shift data recorded for compounds **1**-**4**[a]

Compound	δ_C					
LGO (**1**)	188.9	148.4	126.6	101.5	71.3	66.5
iso-LGO (**3**)	194.5	147.3	127.1	96.1	79.6	62.7
Cyrene™ (**2**)	200.4	101.4	73.1	68.1	30.8	29.8
iso-Cyrene (**4**)	205.6	100.9	79.3	67.2	31.5	30.7

[a] All spectra recorded in $CDCl_3$ at 100 MHz

In the infra-red spectrum of Cyrene® two carbonyl absorption bands are observed at 1724 and 1741 cm^{-1} while a single one (at 1733 cm^{-1}) is observed in the corresponding spectrum of *iso*-Cyrene. This difference reinforces the distinct relationship between the ketone carbonyl groups in each compound and the proximate (in the case of Cyrene®) or remote (in the case of *iso*-Cyrene) internal acetal. Specifically, the 'splitting" of the carbonyl absorption band in Cyrene® can be attributed to the distinct dipole-dipole interactions between the ketone carbonyl and the conformationally locked, axially- and equatorially-oriented C–O bonds of the adjacent internal acetal moiety.[21] The specific rotation $\{[\alpha]_D\}$ reported[9a] for compound **2**[9a] is –246 (c = 0.4, $CHCl_3$) while that recorded, during the course of this work, for congener **4** is of the same sign but significantly smaller in magnitude [–79.1 (c = 0.91, $CHCl_3$)].

The 70 eV electron-impact mass spectrum of *iso*-Cyrene (**4**) revealed a weak molecular ion (10% of base peak) at *m/z* 128 and a cluster of major fragment ions at *m/z* 86 (81%), 85 (base peak) and 84 (80%). The formation of the latter species probably arises through the fragmentation pathway shown in Scheme 3 and wherein the molecular ion **14** (*m/z* = 128) undergoes heterolytic fission of the C1-C2 bond with the resulting radical cation losing the elements of ketene (MW = 42) to afford the 1,3-dioxole **15** (*m/z* = 86) that itself losses a hydrogen atom and so producing the 2-methylene-1,3-dioxolane cation **16** (*m/z* = 85). Finally, loss of a second hydrogen would deliver the 2-methylene-1,3-dioxole radical cation **17** (*m/z* = 84).

Scheme 3: Possible fragmentation pathways operating during the EI-induced mass spectral analysis of *iso*-Cyrene (**4**).

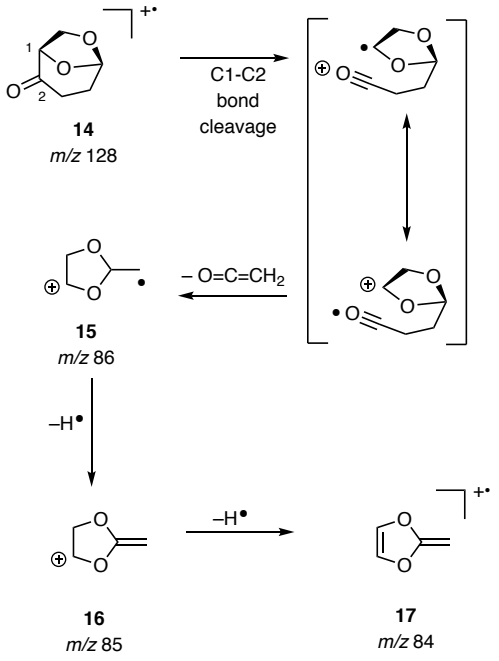

Key Physical Properties of* iso-*Cyrene

The experimentally determined density of *iso*-Cyrene at 22 °C was 1.29 g/mL (± ca. 3%), a value that compares with 1.25 g/mL reported[5] for Cyrene®. Attempts to establish the boiling point of *iso*-Cyrene were conducted at ca. 743 mm Hg (Canberra altitude is ca. 600 m) using DSC techniques. This led to the identification, as shown in Figure S4 of the SI, of a transition point at ca. 117 °C that we take to signify the onset of a decomposition event, the details of which remain to be established. In keeping with such observations, prolonged heating of solutions of the compound in $(CD_3)_2SO$ led to the formation of a dark-yellow coloration while analogous heating of neat material resulted in it developing a distinct brown color. More specifically, while heating a $(CD_3)_2SO$ solution of compound **4** at 120 °C for 1 h did not led to any noticeable change in the ^1H NMR spectrum of the material, after 18 h no resonances due to *iso*-Cyrene could be detected. An experimentally determined boiling point of 220 °C (presumably recorded at 760 mm Hg) has been reported for Cyrene® while the theoretically predicted (ex. CAS) boiling point for *iso*-Cyrene (**4**) is 227.3 (± 25 °C) at 760 mm Hg.

In keeping with expectations, *iso*-Cyrene proved to be entirely miscible, at 22 °C, with equal volumes of cyclohexane, diethyl ether, THF, dichloromethane, ethyl acetate, DMSO, DMF, Cyrene® and NMP. In contrast, it did not mix with water and ^{1}H NMR titration experiments indicated that, unlike its isomer **2**,[12b] *iso*-Cyrene (**4**) does not form a hydrate even when diluted in a 1:10 *v/v* ratio and allowed to stand at ambient temperatures for > 72 h.

Preliminary Studies on the Chemical Reactivity of* iso-*Cyrene

The differences between the chemical behaviors of the LGO (**1**)/Cyrene® (**2**) pair and their isomeric counterparts **3** and **4**, respectively, are quite conspicuous. For example, unlike LGO (**1**), *iso*-LGO (**3**) does not undergo ready conjugate addition of the elements of water (cf. conversion **1** → **5** in Scheme 1) and nor does it readily form dimers (cf. conversion **1** → **6** in Scheme 1). Similarly, unlike Cyrene® (**2**),[22] isomer **4** does not undergo ready self- or trans-aldol-type reactions in the presence of, for example, the base K_3PO_4. In terms of its acid-stability, it has been stated[5] that Cyrene® can be "heated with trifluoracetic acid at 60 °C for 18 h without apparent change". Likewise, when *iso*-Cyrene (**4**) is treated under the same conditions, no chemical change, as assessed by ^{1}H NMR spectroscopic analysis, is observed. In contrast, treatment of compound **4** with 2 M aqueous HCl at ambient temperatures for several hours resulted in notable decomposition and the appearance, in the ^{1}H NMR spectrum of the product mixture, of a resonance attributable to an aldehyde. Analogous treatment of congener **2** only appeared to effect addition of water to the carbonyl moiety and so delivering the corresponding and previously reported[12b] geminal diol (see SI for relevant ^{1}H NMR spectroscopic analyses).

Computational Studies

In an effort to quantify the difference in polarity between congeners **2** and **4**, the dipole moment of each was calculated using density functional theory (see Experimental and SI for details). The outcomes of these calculations, together with those obtained on the unsaturated precursors **1** and **3**, are shown in Table 3. Thus, Cyrene® (**2**) has a significantly higher dipole moment than *iso*-Cyrene (**4**) but both are lower than those of their corresponding unsaturated counterparts. These variations seem intuitively reasonable and consistent with the aligned (in the case of **2**) or opposing (in the case of **4**) acetal and ketone carbonyl residues in these systems. Of course, the introduction of the conjugated C-C double bond into these systems, as

manifest in compounds **1** and **3**, increases the dipole moment of each. This increase in polarity is also clear in the electrostatic potential surfaces of compounds **1**-**4**, as determined in the gas phase at the M06-2X/6-31+G(d,p) level of theory, which are shown in Figure 2.

Table 3: The Calculated Dipole Moments of Compounds **1**-**4**

Compound #	**1**	**2**	**3**	**4**
Structure[a]	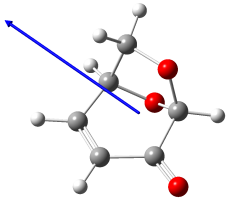	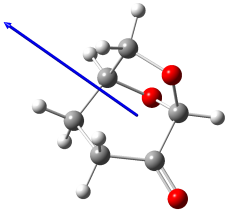	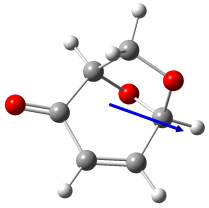	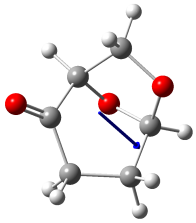
Dipole Moment (Debye)[b]	4.69	4.40	2.09	1.79

[a] Structures shown were produced using GaussView 6

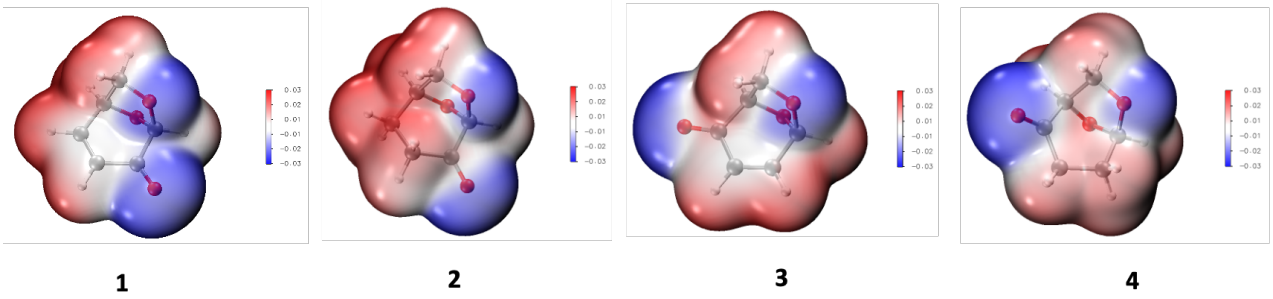

Figure 2: Electrostatic potential surfaces (ESPs) of compounds **1**-**4**, as calculated at the M062X/6-31+G(d,p) level of theory (in the gas phase).

COSMO-RS calculations[23] were also used to understand the solvation properties of Cyrene® and *iso*-Cyrene (and compared to NMP for reference). The molecular size and surface charges of *iso*-Cyrene are very similar to Cyrene® (as determined with COSMO-RS at the B88-VWN-PB86/TZVP level of theory, see SI, Figure S5). This suggests *iso*-Cyrene could take the place of Cyrene® in solvent substitutions despite its smaller dipole moment, which is particularly useful where miscibility and reactivity with water is undesirable. *iso*-Cyrene and Cyrene® are calculated not to interact as strongly with positive charges as NMP and other conventional dipolar aprotic solvents. This may limit applications requiring the stabilisation of charges or the solubility of salts.

Biological Properties

In vitro *toxicological profiling*

Cyrene® (**2**) is widely reported to offer reduced toxicity in comparison to common *N*-containing polar aprotic solvents such as NMP, *N,N*-dimethylformamide (DMF) and *N,N*-dimethylacetamide (DMAc).[2,6] Toxicological evaluations of emerging new solvents that conform to regulatory guidelines and involve conventional animal tests remain a challenge since large quantities of ultra-pure sample are required. They are also time-consuming and costly. As such, the rapid *in vitro* assessment of neoteric solvents is an ideal alternative for initial assessments of toxicity and thus reducing the risk of "regrettable substitutions".[24] Accordingly, *iso*-Cyrene (**4**) was analyzed using a panel of eleven CALUX® *in vitro* reporter gene assays, covering different toxicological endpoints. These CALUX assays specifically detect the ability of a test compound to modulate a certain nuclear receptor (ERα, AR, TRβ, PPARγ, PXR and AhR CALUX) or a cell signaling pathway (AP-1, ESRE, Nrf2 and p53 CALUX). The assays have been used successfully in several large screening programs, such as the EU Framework program (FP) projects ReProTect, ChemScreen and EU-ToxRisk.[25-31] Additionally, they have been applied to safety assessments of bio-based solvents[32] and bio-based plasticizers.[33] The assays selected for the present study cover a broad range of toxicological endpoints, including endocrine activity (ERα, AR, TRβ), xenobiotic sensing (PXR, AhR), oxidative stress (Nrf2), protein unfolding (ESRE) and DNA damage/genotoxicity (AP-1, p53).

The lowest effective concentrations (LOECs) in LogM observed for Cyrene® (**2**) and *iso*-Cyrene (**4**) in all eleven *in vitro* assays are shown in Table 4. Both compounds have remarkably similar profiles, indicating that these regioisomers differ little in their *in vitro* activity. Cyrene® (**2**) was previously been shown to be non-mutagenic and non-ecotoxic.[6] The present study reveals that Cyrene® (**2**) shows slight cytotoxicity and activates two cellular stress pathways (AP-1: cell cycle control and Nrf2: oxidative stress) but such activation takes place at concentrations 2-6 orders of magnitude higher than the LOECs of the assays' reference compounds (top row) and indicating a low potency. Since the *in vitro* profile of *iso*-Cyrene (**4**) on the eleven CALUX assays was virtually identical, there is no indication that it has a less favorable toxicological profile.

Table 4: *In vitro* CALUX reporter gene assay results for Cyrene™ (**2**) and *iso*-Cyrene (**4**)[a]

Compound	Cytotox 20%	ERα	AR-anti	TRβ-anti	PPARγ	PXR	AhR	AP-1	ESRE	Nrf2	p53
Assay references	–6.6	–12.2	–7.7	–6.9	–7.7	–7.1	–12.3	–9.5	–7.5	–5.4	–9.0
Cyrene™ (**2**)	–3.2	>	>	>	>	>	>	–3.3	>	–3.5	>
iso-Cyrene (**4**)	–3.1	>	>	>	>	>	>	–2.0	>	–3.5	>

[a]*In vitro* results are presented as lowest observed effect concentrations (LOECs) in LogM; '>': no activity detected up to the highest tested concentration. 'N/A': not analyzed; Top row: LOECs of each assay's positive control reference compound. Cells are color-coded based on the LOECs: green = LOEC > [max analysed]; light orange = LOEC >-4; orange = LOEC <-5;

Gas chromatographic-olfactometry (GC-O) analysis

Pure Cyrene® (**2**) was evaluated by perfumers and flavorists and described as having bacon, smoked and vanilla notes. In contrast, olfactory evaluation of *iso*-Cyrene (**4**) performed by trained panelists revealed only sulfury and unpleasant olfactive notes and these are attributed to the introduction of contaminants during the Swern oxidation step associated with the synthetic sequence outlined in Scheme 1. Accordingly, gas chromatographic-olfactometry (GC-O) analysis[34] (Figure 3) was then performed to specifically assess the odor of the compounds (Table 5). By such means, Cyrene® (**2**) eluting between 5.54 and 5.80 min proved to smell exactly as expected with a better appreciation of the vanilla note on the GC-O. On the other hand, no odor was detected between 4.95 and 5.10 min of retention time which correspond to the elution of the peak of the *iso*-Cyrene (**4**). Sulfury notes were detected on compounds barely responsive to FID.

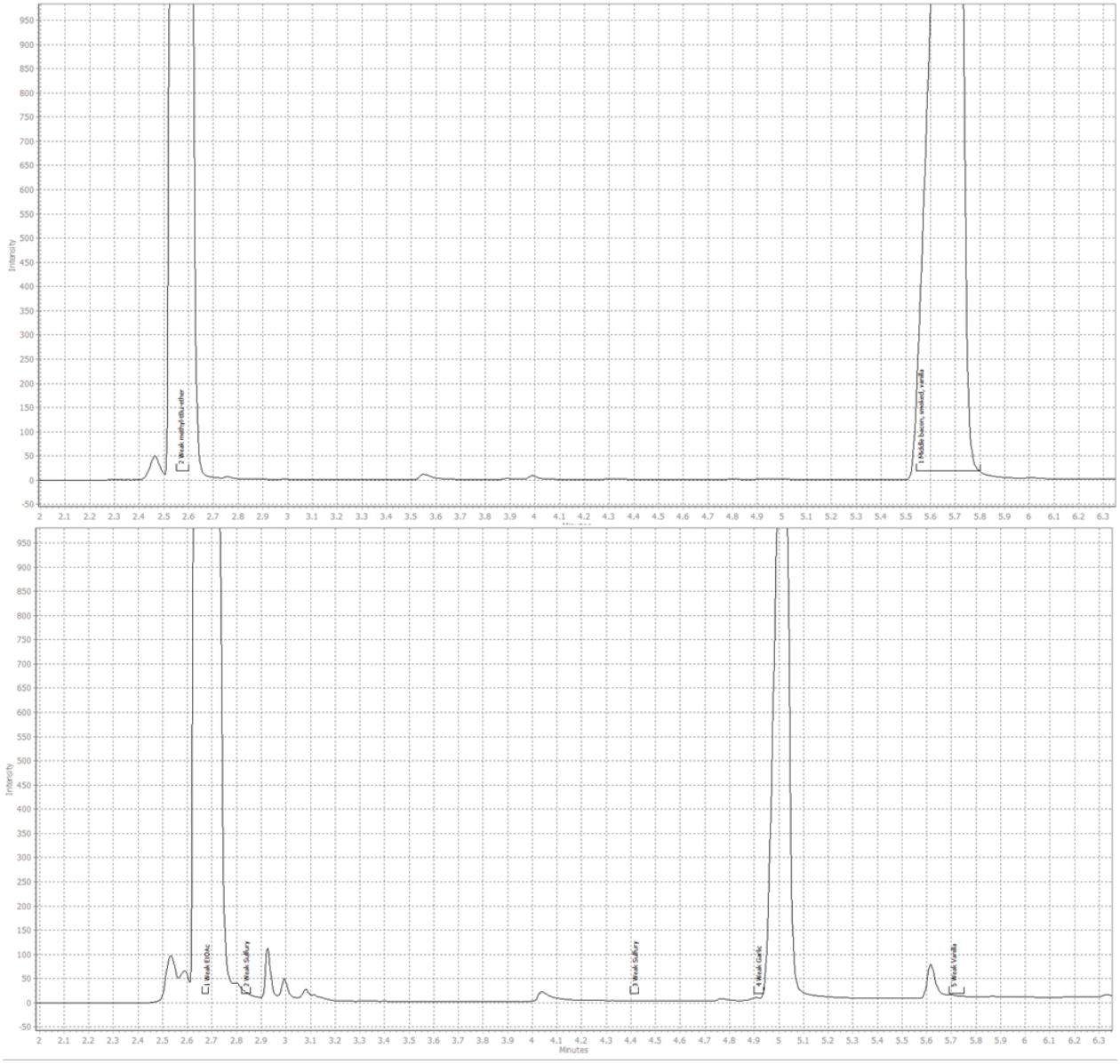

Figure 3: GC-O analysis of Cyrene® (**2**) (top) and *iso*-Cyrene (**4**) (bottom). Markers were placed during the analysis when an odor was detected. The earlier eluting and major peak in each chromatogram is due to the diluting solvent, this being either methyl *tert*-butyl ether (top) or ethyl acetate (bottom).

Table 5: Retention time and odor description obtained during GC-O analysis of a sample of Cyrene® (**2**) and of *iso*-Cyrene (**4**).

Sample	Retention time (min)	Odor	Intensity
Cyrene®	2.54-2.60	methyl *tert*-butyl ether (dilution solvent)	Weak
	5.54-5.80	bacon, smoked, vanilla	Medium
***iso*-Cyrene**	2.65-2.69	ethyl acetate (dilution solvent)	Weak
	2.81-2.85	sulfury	Weak
	4.39-4.42	sulfury	Weak
	4.90-4.92	garlic	Weak
	5.68-5.73	vanilla	Weak

Conclusions

These studies reported here reveal that there are significant enough differences in the properties of the sustainably-derived Cyrene® (**2**) and isomer **4** (*iso*-Cyrene) to suggest they will exert complementary effects as solvents in a range of settings. These differences are due, in large part, to the relative positioning of the ketone and acetal residues within the associated bicyclic frameworks. In compound **2** the adjacent location of these functionalities increases the electrophilicity of the carbonyl moiety and the acidity of the hydrogens associated with the α-methylene unit. Likewise, the acid-stability of the acetal group is increased by the presence of the neighboring and electron-withdrawing ketone residue. In compound **4** there is significantly less interaction between the equivalent residues and such that they behave much like "normal" (isolated) ketone and acetal groups. As a consequence, Cyrene® (**2**) is likely to be somewhat less acid sensitive than isomer **4** (*iso*-Cyrene) while the latter is less base sensitive. These same structural differences also dictate (and explain) the differing miscibilities of the compounds with water. As detailed above, *in vitro* testing suggests compounds **2** and **4** have similar and favorable toxicological properties. That said, the lack of an odor associated with *iso*-Cyrene (**4**) may confer some advantages in terms of its exploitation as solvent although doing so would require the development of superior means of preparing it. Regardless of how this might be achieved, this work reinforces the significant value of LGO (**1**) as a bio-derived platform molecule.[35]

Experimental

General Experimental Procedures

Unless otherwise specified, proton (^{1}H) and carbon (^{13}C) NMR spectra were recorded at 18 °C in base-filtered $CDCl_3$ on a Varian spectrometer operating at 400 MHz for proton and 100 MHz for carbon nuclei. For ^{1}H NMR spectra, signals arising from the residual protio-forms of the solvent were used as the internal standards. ^{1}H NMR data are recorded as follows: chemical shift (δ□□□multiplicity, coupling constant(s) *J* (Hz), relative integral] where multiplicity is defined as: s = singlet; d = doublet; t = triplet; q = quartet; m = multiplet or combinations of the above. The signal due to residual $CHCl_3$ appearing at δ_H 7.26 and the central resonance of the $CDCl_3$ "triplet" appearing at δ_C 77.2 were used to reference ^{1}H and ^{13}C NMR spectra, respectively. Infrared spectra (ν_{max}) were recorded on a Perkin-Elmer 1800 Series FTIR Spectrometer. Samples were analyzed as thin films on KBr plates. Low-resolution ESI mass spectra were recorded on a Micromass LC-ZMD single quadrupole liquid chromatograph-mass spectrometer while high-resolution measurements were conducted on an LCT Premier time-of-flight instrument. Low- and high-resolution EI mass spectra were recorded on an Autospec Premier Micromass magnetic-sector machine. Optical rotations were recorded in $CHCl_3$ at 20 °C on a Perkin Elmer Model 343 Polarimeter. Melting points were measured on an Optimelt automated melting point system and are uncorrected. Analytical thin layer chromatography (TLC) was performed on aluminum-backed 0.2 mm thick silica gel 60 F_{254} plates as supplied by Merck. Eluted plates were visualized using a 254 nm UV lamp and/or by treatment with a suitable dip followed by heating. These dips included phosphomolybdic acid : ceric sulfate : sulfuric acid (conc.) : water (37.5 g : 7.5 g : 37.5 g : 720 mL) or potassium permanganate : potassium carbonate : 5% sodium hydroxide aqueous solution : water (3 g : 20 g: 5 mL : 300 mL). Flash chromatographic separations were carried out following protocols defined by Still *et al*.[36] with silica gel 60 (40-63 □m) as the stationary phase and using the AR- or HPLC-grade solvents indicated. Starting materials and reagents were generally available from the Sigma-Aldrich, Merck, TCI, Strem or Lancaster Chemical Companies and were used as supplied. Drying agents and other inorganic salts were purchased from the AJAX, BDH or Unilab Chemical Companies. Tetrahydrofuran (THF), methanol and dichloromethane were dried using a Glass Contour solvent purification system that is based upon a technology originally described by Grubbs *et al*.[37] Where necessary, reactions were performed under an inert atmosphere.

Specific Synthetic Transformations

(1*R*,2*S*,5*R*)-2-Hydroxy-6,8-dioxabicyclo[3.2.1]octan-4-one (5) and Dimer 6. A magnetically stirred solution of levoglucosenone (**1**) (5.94 g, 47.1 mmol) in water (470 mL) maintained at 22 °C was treated with triethylamine (4.70 mL, 3.72 mmol). After 1 h the reaction mixture was concentrated under reduced pressure and the ensuing residue subjected to flash chromatography (silica, 1:10 v/v ethyl acetate/40-60 petroleum ether → ethyl acetate gradient elution) and so affording two fractions, A and B.

Concentration of fraction A (R_f = 0.3) gave a solid that on recrystallization (CH_2Cl_2) afforded dimer **6**[15] (64 mg, 0.5%) as white, crystalline solid, m.p. = 163-165 °C (lit.[15a] m.p. = 170-172 °C), $[\alpha]_D$ = –444 (*c* 0.49, acetone) {lit.[15a] $[\alpha]_D$ = –482 (*c* 0.3, acetone)}. ^{1}H NMR (400 MHz, $CDCl_3$) δ 7.11 (d, *J* = 6.0 Hz, 1H), 5.43 (s, 1H), 5.14 (s, 1H), 5.09 (m, 1H), 4.55 (m, 1H), 4.18 (d, *J* = 8.4 Hz, 1H), 4.06 (m, 1H), 3.91 (m, 1H), 3.73 (d, *J* = 6.8 Hz, 1H), 3.46 (d, *J* = 8.4 Hz, 1H), 3.00 (dd, *J* = 17.6 and 8.4 Hz, 1H), 2.25 (d, *J* = 17.6 Hz, 1H); ^{13}C{^{1}H} NMR (100 MHz, $CDCl_3$) δ 200.2, 188.3, 143.9, 137.2, 101.8, 101.1, 75.1, 72.4, 68.3, 66.5, 38.6, 35.1; IR ν_{max} 2971, 2902, 1729, 1686, 1120, 1097, 981, 968, 906, 896, 867, 844, 819, 670 cm^{-1}; MS (EI, 70 eV) *m/z* 252 ($M^{+\bullet}$, <1%), 224 (<1), 149 (78), 105 (100), 91 (77), 79 (60); HRMS (EI, 70 eV) calcd for $C_{12}H_{12}O_6$ ($M^{+\bullet}$) 252.0628, found 253.0623.

Concentration of fraction B (R_f = 0.2) gave compound **5**[8] (4.88 g, 72%) as a clear, light-yellow oil that was identical, in all respects, with material obtained earlier.[8]

(1*R*,2*S*,4*S*,5*R*)-4-(Dimethylamino)-6,8-dioxabicyclo[3.2.1]octan-2-ol (4*S*-7) and (1*R*,2*S*, 4*R*,5*R*)-4-(Dimethylamino)-6,8-dioxabicyclo[3.2.1]octan-2-ol (4*R*-7). A magnetically stirred solution of compound **5** (4.00 g, 27.8 mmol), prepared as described immediately above, and dimethylamine (10 mL of a 40% aqueous solution, 83.0 mmol) in methanol (140 mL) maintained at 22 °C was treated with 10% palladium on carbon (200 mg). The resulting mixture was placed under a balloon of hydrogen and after 24 h the reaction mixture was filtered through a pad of diatomaceous earth and the filtrate concentrated under reduced pressure. The resulting oil was dissolved into dichloromethane (200 mL) then dried (Na_2SO_4) and filtered before being concentrated under reduced pressure to give compound **7** (4.40 g, 92%) as a clear, yellow oil and *ca*. 3:1 mixture of epimers. ^{1}H NMR (400 MHz, $CDCl_3$) δ 5.61 (s, 0.75H), 5.57 (s, 0.25H), 4.48 (broad s, 1H), 3.92-3.76 (complex m, 3H), 2.75 (m, 1H), 2.38 (s, 6H), 1.98 (m, 1H), 1.98-1.90 (complex m, 1H), 1.87-1.80 (complex m, 1H); ^{13}C NMR (100 MHz, $CDCl_3$) δ 101.0 (major isomer), 100.7 (minor isomer), 78.4, 67.8, 67.3, 66.6, 66.4,

63.7, 61.4, 44.1, 42.0, 27.5, 25.8; IR ν_{max} 3368, 2953, 2892, 2827, 2783, 1458, 1131, 1037, 1002, 901, 861, 781, 688, 483 cm^{-1}; MS (ESI, +ve) *m/z* 222 (100%), 174 [$(M+H)^+$, 90]; HRMS calcd for $C_8H_{16}NO_3$ [$(M+H)^+$] 174.1130, found 174.1127.

(1*R*,5*R*)-6,8-Dioxabicyclo[3.2.1]oct-3-en-2-one (3), (1R,5R)-4-(Dimethylamino)-6,8-dioxabicyclo[3.2.1]octan-2-one (8) and (1R,4R,5R)-4-(Methylthio)-6,8-dioxabicyclo[3.2.1]-octan-2-one (9). A solution of DMSO (1.88 g, 24 mmol) in dichloromethane (20 mL) was added, dropwise *via* syringe, to a magnetically stirred solution of oxalyl chloride (1.52 g, 12 mmol) in dichloromethane (30 mL) maintained at –70 °C. The ensuing mixture was allowed warm to –58 °C then re-cooled to –70 °C over a 0.25 h period. Thereafter, a solution of amino-alcohol **7** (1.73 g, 10 mmol) in dichloromethane (30 mL) was added to the reaction mixture over 10 min. After a further 0.75 h, triethylamine (5.58 mL, 40 mmol) was added to the reaction mixture over 5 min. After this time, the reaction mixture was allowed to slowly warm to –5 °C and then filtered through a pad of diatomaceous earth contained in a sintered glass funnel. The filtrate was concentrated under reduced pressure to afford a malodorous, light-yellow oil comprised of a mixture of compounds **3**, **8** and **9**.

In order to obtain a sample of the last compound for the purposes of spectroscopic characterization, this oil was subjected to flash chromatography (silica, 1:10 v/v ethyl acetate/petroleum ether elution) and so affording, after concentration of the relevant fractions (R_f = 0.2), compound **9** (226 mg, 13%) as a foul-smelling, yellow oil, $[\alpha]_D$ = –23.6 (*c* = 0.06, $CHCl_3$). ^1H NMR (400 MHz, $CDCl_3$) δ 5.69 (s, 1H), 4.54 (d, *J* = 5.4 Hz, 1H), 3.96 (d, *J* = 8.1 Hz, 1H), 3.86 (dd, *J* = 8.1 and 5.4 Hz, 1H), 3.02 (m, 1H), 2.85 (m, 1H), 2.52 (dd, *J* = 17.5 and 4.8 Hz, 1H), 2.18 (s, 3H); ^{13}C NMR (100 MHz, $CDCl_3$) δ 204.7, 103.8, 79.2, 67.1, 45.4, 39.0, 13.9; IR ν_{max} 2963, 2896, 1732, 1668, 1406, 1173, 1114, 1010, 894, 793, 754 cm^{-1}; MS (ESI, +ve) 229 [$(M+MeOH+Na)^+$, 100%]; MS (EI, +ve) *m/z* 174 ($M^{+\bullet}$, 50%), 74 (100); HRMS calcd for $C_7H_{10}O_3S$ ($M^{+\bullet}$) 174.0351, found 174.0347.

The high polarity of the presumed primary oxidation product **8** as well as its seeming propensity to engage in (possibly) Schiff-base-type condensation and other reactions thwarted efforts to obtain it in pure form.

Conversion of Amino-ketone 8 into *iso*-LGO (3). A magnetically stirred solution of the crude product obtained, as described immediately above, from the Swern oxidation of amine **7** in THF (50 mL) and maintained at 22 °C was treated with methyl iodide (1.2 mL, 20 mmol) and potassium carbonate (2.70 g, 20 mmol). After 18 h the reaction mixture was filtered

through a pad of diatomaceous earth and the filtrate concentrated under reduced pressure. The residue so obtained was subjected to flash chromatography (silica, 1:10 v/v ethyl acetate/petroleum ether elution) and concentration of the relevant fractions (R_f = 0.2) gave compound **3**[8a] (617 mg, 49%) as a clear, yellow oil. This material was identical, in all respects, with that obtained earlier.[8a]

(1*R*,5*R*)-6,8-Dioxabicyclo[3.2.1]octan-2-one (*iso*-Cyrene, 4). A magnetically stirred mixture of *iso*-LGO (**3**) (2.56 g, 20 mmol) and W2 Raney Ni (*ca*. 200 mg) in THF (100 mL) maintained at 22 °C was placed under a balloon of hydrogen. After 24 h an externally applied magnet was used to retain the solid catalyst within the reaction flask while the supernatant liquid was decanted into another vessel. The retained solids were washed with ethyl acetate (2 × 30 mL) (CAUTION: the washed solid should be treated with water so as to prevent combustion). The combined organic phases were concentrated under reduced pressure to give a clear, colorless oil that was subjected to flash column chromatography (silica, 1:10 v/v ethyl acetate/ petroleum ether elution). Concentration of the relevant fractions (R_f = 0.1) gave an oil that was subject to distillation at reduced pressure and thus affording *iso*-Cyrene (**4**)[9,10] (1.89 g, 74%) as a clear, colorless oil of undefined boiling point, $[\alpha]_D$ = –79.1 (*c* = 0.91, $CHCl_3$) {lit.[9a] $[\alpha]_D$ = –83 (*c* = 0.8, $CHCl_3$)}. ^{1}H NMR (400 MHz, $CDCl_3$) δ see Table 1; ^{13}C NMR (100 MHz, $CDCl_3$) δ see Table 2; IR ν_{max} 2963, 1733, 1118, 1008, 1017, 995, 871 cm^{-1}; MS (EI, +ve) *m/z* 128 ($M^{+\bullet}$, 10%), 86 (81), 85 (100), 84 (80); HRMS calcd for $C_6H_8O_3$ ($M^{+\bullet}$) 128.0473, found 128.0473.

(3a*R*,5*S*,6*S*,6a*R*)-5-((*R*)-2,2-Dimethyl-1,3-dioxolan-4-yl)-2,2-dimethyltetrahydrofuro[2,3-*d*][1,3]dioxol-6-ol (11): Phosphoric acid (1.0 mL of an 85% solution in water) was added, dropwise, to magnetically stirred, anhydrous acetone (300 mL) and the resulting solution was treated with a well-dried and finely powdered mixture of *D*-glucose (**10**) (30.0 g) and anhydrous zinc chloride (26.0 g). Stirring was continued for 30 h at 22 °C before the reaction mixture was cooled in an ice-bath then basified (to pH 8) through the portion-wise addition of sodium hydroxide (1 M aqueous solution) while ensuring the temperature of the reaction mixture did not exceed 15 °C. The precipitated mass, comprising sodium sulfate, zinc chloride and unreacted *D*-glucose (**10**), was removed by filtration and the solids thus retained washed with acetone. The combined filtrates were concentrated under reduced pressure and the solid residue recrystallized (*n*-hexane) to give, after hot filtration then cooling, bis-acetonide **11**[38] (32.0 g, 74%) as a white, crystalline solid, m.p. = 104-105 °C (lit.[38] m.p. =

111-112 °C), $[\alpha]_D$ = –5.88 (*c* 0.17, acetone). ^{1}H NMR (400 MHz, $CDCl_3$) δ 5.95 (d, *J* = 3.6 Hz, 1H), 4.54 (d, *J* = 3.6 Hz, 1H), 4.38-4.30 (complex m, 2H), 4.17 (dd, *J* = 8.8 and 6.4 Hz, 1H), 4.07 (dd, *J* = 7.6 and 2.8 Hz, 1H), 3.97 (dd, *J* = 8.8 and 5.2 Hz, 1H), 1.50 (s, 3H), 1.44 (s, 3H), 1.36 (s, 3H), 1.32 (s, 3H) ; ^{13}C NMR (100 MHz, $CDCl_3$) δ 111.8, 109.7, 85.1, 81.1, 75.3, 73.5, 67.7, 26.9, 26.8, 26.2, 25.1.

(3a*R*,5*R*,6*S*,6a*R*)-5-((*R*)-2,2-Dimethyl-1,3-dioxolan-4-yl)-2,2-dimethyltetrahydrofuro[2,3-*d*][1,3]dioxol-6-yl 4-Methylbenzenesulfonate (12): A solution of compound **11** (11.8 g, 45.3 mmol) and *p*-toluenesulfonyl chloride (17.3 g, 90.7 mmol) in pyridine (20 mL) was allowed to stand at 22 °C for 24 h then poured, with stirring, into ice-water (150 mL) and the resulting solid filtered off, washed several times with water then dried and recrystallized (methanol) to give compound **12**[39] (16.2 g, 86%) as a white crystalline solid, m.p. = 119-120 °C (lit.[39a] m.p. = 119-120 °C), $[\alpha]_D$ = –51.7 (*c* 0.2, acetone). ^{1}H NMR (400 MHz, $CDCl_3$) δ 7.84 (d, *J* = 8.4 Hz, 2H), 7.33 (d, *J* = 8.4 Hz, 2H), 5.92 (d, *J* = 3.6 Hz, 1H), 4.83 (d, *J* = 3.6 Hz, 1H), 4.79 (broad s, 1H), 4.08-3.95 (complex m, 3H), 3.90 (m, 1H), 2.45 (s, 3H), 1.48 (s, 3H), 1.31 (s, 3H), 1.20 (s, 3H), 1.15 (s, 3H); ^{13}C NMR (100 MHz, $CDCl_3$) δ 145.2, 132.8, 129.8, 128.6, 112.7, 109.2, 105.3, 83.5, 82.2, 80.0, 71.9, 67.3, 26.8, 26.4, 25.1, 21.8

(3a*R*,6a*R*)-5-((*R*)-2,2-Dimethyl-1,3-dioxolan-4-yl)-2,2-dimethyl-3a,6a-dihydrofuro[2,3-*d*]-[1,3]dioxole (13): The conditions reported by Horton[19] and by Norris[40] for forming alkene **13** from tosylate **12** (7.3 g, 17.6 mmol) (by treating the latter with *t*-BuOK in THF) were employed on multiple occasions in the present study and in each instance a waxy-yellow solid was obtained after work-up. NMR spectroscopic analysis of this material suggested it contained varying mixtures of the starting ester (**12**) and the target alkene **13**[19,40] alongside other, unidentified components. All attempts to purify product **13** by chromatographic means failed. Accordingly, the waxy-solid obtained after work-up was subjected to treatment with aluminum chloride as detailed immediately below.

***iso*-LGO (3)**. Following the procedure of Horton,[19] anhydrous aluminum chloride (390 mg, 2.95 mmol) was added to a vigorously stirred mixture of dry diethyl ether (30 mL) and pentane (22 mL) that had been cooled to 0 °C under an argon atmosphere. A solution of the waxy-solid (1.43 g, 5.90 mmol) obtained from the preceding step (see immediately above) in diethyl ether (6 mL) was then added dropwise over a 2 min. and the resulting mixture was stirred for an additional 7 min at 0 °C and then quickly transferred to a flash chromatography

column (25 mm i.d.) containing a 4 cm deep pad of silica gel. The reaction mixture was rapidly forced through the apparatus using compressed air and pad then washed with diethyl ether/pentane (1:1 v/v mixture) until no more UV-active material could be detected (by TLC) in the column eluent (ca. 300 mL required). The combined filtrates were concentrated under reduced pressure to afford a brown syrup that was subjected to flash chromatography (silica, 5:1 v/v pentane/diethyl ether elution) to give, after concentration of the relevant fractions (R_f = 0.2), compound **3**[8a] (60 mg, 8%) as a pale-yellow syrup. ^{1}H and ^{13}C NMR spectroscopic analysis of this material revealed that is was contaminated with a tosyl-containing species.

Crystallographic Studies

Crystallographic Data

Compound **6**. $C_{12}H_{12}O_6$, M = 252.22, T = 150 K, monoclinic, space group $P2_1$, Z = 4, a = 6.60390(10) Å, b = 18.9253(2) Å, c = 9.27500(10) Å; β = 107.663(2); V = 1104.55(3) Å^3, D_x = 1.517 Mg m^{-3}, 4431 unique data ($2\theta_{max}$ = 147.642°), R = 0.0579 [for 4385 reflections with $I > 2.0\sigma(I)$]; Rw = 0.0237 (all data), S = 1.055.

Compound **11**. $C_{12}H_{20}O_6$, M = 260.28, T = 150 K, monoclinic, space group C2, Z = 8, a = 20.7196(6) Å, b = 5.5609(2) Å, c = 24.6708(8) Å; β = 110.883(4); V = 2655.83(16) Å^3, D_x = 1.302 Mg m^{-3}, 4465 unique data ($2\theta_{max}$ = 133.172°), R = 0.0465 [for 4224 reflections with $I > 2.0\sigma(I)$]; Rw = 0.1218 (all data), S = 1.076.

Compound **12**. $C_{19}H_{26}O_8S$, M = 414.46, T = 150 K, orthorhombic, space group $P2_12_12_1$, Z = 4, a = 9.79882(18) Å, b = 10.1911(3) Å, c = 21.2482(5) Å; V = 2121.86(9) Å^3, D_x = 1.297 Mg m^{-3}, 3883 unique data ($2\theta_{max}$ = 136.494°), R = 0.0325 [for 3539 reflections with $I > 2.0\sigma(I)$]; Rw = 0.0833 (all data), S = 1.040.[20]

Structure Determinations

Data for compounds **6**, **11** and **12** were collected on a a Rigaku Super Nova X-ray diffractometer employing CuKα radiation and a graphite monochromator (λ = 1.54184 Å). Using OLEX2,[41] the structures were solved by direct methods with the ShelXT[42] program and refined, using least squares minimization, with the ShelXL[43] package. Atomic coordinates, bond lengths and angles, and displacement parameters have been deposited at the Cambridge Crystallographic Data Centre (CCDC nos. 2079098 and 2092948). These data can be obtained

free-of-charge via www.ccdc.cam.ac.uk/data_request/cif, by emailing data_request@ccdc.cam.ac.uk, or by contacting The Cambridge Crystallographic Data Centre, 12 Union Road, Cambridge CB2 1EZ, UK; fax: +44 1223 336033.

Determination of Certain Physical Properties of *iso*-Cyrene

Miscibility and Degree of Hydration

For miscibility studies, equivalent volumes (ca. 5-10 □L) of *iso*-Cyrene and the relevant "co-solvent" were loaded into melting point tubes *via* micropipette. The loaded tubes were quickly inverted several times and then allowed to stand at 22 °C for 0.5 h. After this time the tubes were loaded into a melting point apparatus incorporating a magnifying aperture and the contents of the tube inspected for the presence or absence of an interface between phases. Only in the case of the water/*iso*-Cyrene mixture was such an interface observed.

For the degree of hydration study, and following protocols used by Camp *et al*,[12b] an aliquot of *iso*-Cyrene was allowed to stand as a mixture with ten v/v equivalents of D_2O at ambient temperatures prior to analysis, at regular intervals up to 72 h, by ^1H NMR spectroscopy. No evidence for the formation of a hydrate analogous to that observed for Cyrene® was observed at any stage.

Density

Using micro-pipetting techniques, a defined volume (ca. 20 □L) of *iso*-Cyrene was placed in a tared melting point tube and its weight determined, at 22 °C, using a micro-balance. Triplicate experiments gave an average density of 1.29 g/mL (± 3%). This compares with a value of 1.25 g/mL reported[5] for Cyrene® at 20 °C.

Attempted Boiling Point Determination

Attempts to determine the boiling point of *iso*-Cyrene (**4**) at ca. 743 mm Hg were undertaken using a TA Instruments Q20 DSC apparatus. A representative trace arising from this type of analysis is shown in Figure S4 (see below). The inflection point observed at *ca*. 117 °C is attributed to decomposition rather than to the boiling of the sample. A boiling point of 116-116.5 °C (at *ca*. 7.5 mm Hg) has been reported[5] for Cyrene®.

Chemical Reactivity Studies

To assess the stability of *iso*-Cyrene in the presence of base, an equivalent mass of tribasic potassium phosphate was intimately mixed with *iso*-Cyrene at *ca*. 22 °C, before being allowed to stand for 18 h. The liquid was then decanted, dissolved in deuterated chloroform and analysed by proton NMR spectroscopy. This revealed that *iso*-Cyrene remained unaffected after exposure to such conditions.

To assess the stability of *iso*-Cyrene in the presence of acid, equal volumes (ca. 10 □L) of each of trifluoroacetic acid, D_2O and *iso*-Cyrene were intimately mixed then heated at 60 °C (oil bath) for 18 h. The resulting mixture was dissolved in $CDCl_3$ and analyzed by ^1H NMR spectroscopy. This revealed that *iso*-Cyrene had not reacted under these conditions. In contrast, treatment of *iso*-Cyrene with a two-fold excess (v/v) of 2 M aqueous HCl at 60 °C for 1 h resulted in significant discoloration. Accordingly, the cooled reaction mixture was diluted with $(CD_3)_2SO$ and the ^1H NMR spectrum of the resulting solution was recorded (see below). This revealed significant decomposition had taken place. An analogous experiment involving Cyrene® did not result in any discoloration and analysis of the corresponding ^1H NMR spectrum (see below) suggested only formation of Cyrene® hydrate had occurred.

Theoretical Studies

All calculations were performed at the M062X/6-31+G(d,p) level of theory using Gaussian G16c01.[44] Dipole moments and electrostatic potential maps were calculated in the gas phase, while SMD solvent corrections in cyclohexane were used to generate the van der Waals and solvent accessible surfaces. Electrostatic potential maps were generated with the Multiwfn program,[45] while GaussView 6[46] was used to plot the dipole moments, and solute-solvent cavities.

Molecular conformations of molecules were calculated with COSMOconfX (version 4.0; COSMOlogic GmbH & Co. KG, Leverkusen, Germany, 2015) while COSMOthermX (version C30_1705; COSMOlogic GmbH & Co. KG, 2017, TZVP basis set level) was used to provide molecular surface charges, σ-profiles, and σ-potentials. COSMO-RS calculations are courtesy of, and authorised for the purposes of, Circa Group Pty Ltd.

Biological Studies

CALUX reporter gene assay methodology

The *in vitro* assessment consisted of the analysis of the solvents against a panel of eleven CALUX® *in vitro* reporter gene assays, covering different toxicological endpoints [agonism on the estrogen (ERα), peroxisome proliferator activated (PPARγ), pregnane-X (PXR) and aryl hydrocarbon (AhR) receptors, antagonism on the androgen (AR) and thyroid (TRβ) receptors, activation of the oxidative stress (Nrf2), unfolded protein response (ESRE), DNA damage (p53) and cell cycle control (AP-1) pathways, and cytotoxicity].

The assays are based on the human osteosarcoma cell line U-2 OS (ATCC HTB-96). Each cell line is stably transfected with a reporter gene plasmid containing luciferase under control of the responsive elements of a specific receptor (e.g. estrogen receptor) or cell signaling pathway (e.g. Nrf2). Activation of the transfected pathway or receptor by a test chemical results in luciferase production, which can be measured as light production by adding the substrate luciferin. Since most nuclear hormone receptors are not endogenously expressed in U-2 OS cells, these receptors were co-transfected when applicable (ERα, AR, TRβ, PXR, AhR, PPARγ).

CALUX cells were routinely subcultured every 3-4 days in growth medium consisting of DMEM (Gibco) supplemented with 7.5% fetal calf serum, 1 × non-essential amino acids (Gibco) and 10 U mL^{-1} penicillin and 10 μg mL^{-1} streptomycin. Cells were maintained at 37 °C under a 5% CO_2 atmosphere. All CALUX assays were performed as described in detail in the publicly available DBALM protocol 197.[47] The assay medium used consisted of DMEM without phenol-red indicator (Gibco) supplemented with 5% DCC-stripped fetal calf serum, 1 × non-essential amino acids (Gibco) and 10 U mL^{-1} penicillin and 10 μg mL^{-1} streptomycin. For seeding, a cell suspension in assay medium was made of 1×10^5 cells mL^{-1}, and the white 384-wells plates were seeded with 30 μL per well cell suspension. After 24 h, cells were exposed to a dilution series of the test compound in DMSO (1% v/v) using a liquid handling robot (ex. Hamilton) coupled to an incubator (Cytomat). The final concentrations of the substances in the wells were 1×10^{-2} to 3×10^{-8} M in 0.5 log unit increments. All samples were tested in triplicate. After 24 h exposure the medium was removed and 10 μL per well Triton-lysis buffer was added. The luciferase signal was then measured in a luminometer (Infinite Pro reader coupled to a Connect stacker, both ex. TECAN Group Ltd).

GC-O Studies

The GC-Olfaction (GC-O) analyses was performed twice by two trained panelists using a Shimadzu GC-2010 Plus instrument equipped with a DB-1MS column (30 m × 0.32 mm × 0.25 μm), a FID detector and a Phaser sniffing port (ex. GL Sciences) and so allowing simultaneous olfactive evaluation and FID peak observation. The split ratio was 4:1 and an AOC-20i auto injector was used. The injection volume was 0.5 μL. Data analysis software including an olfactory voicegram interface kit (ex. GL Sciences) was used.

A sample of Cyrene® (**2**) (18 mg, 0.14 mmol) was diluted in MTBE (0.72 g) and injected into the GC-O instrument. The odor of the Cyrene® peak corresponded to the odor of the pure liquid which is described as "bacon, smoked, vanilla". The vanilla note is more appreciable on the GC-O.

A sample of *iso*-Cyrene (**4**) (36 mg, 0.28 mmol) was diluted in ethyl acetate (1.27 g) and injected into GC-O system. No odor was detected for the *iso*-Cyrene peak.

Supplementary Material

Plots derived from the single-crystal X-ray analyses of compounds **6**, **11** and **12**, trace derived from the DSC analyisis of compound **4** together with copies of the ^{1}H and $^{13}C\{^{1}H\}$ NMR spectra of compounds **3**-**7**, **9**, **11** and **12** as well the ^{1}H NMR spectra of the product mixtures obtained on treating Cyrene® (**2**) and *iso*-Cyrene (**4**) with 2 M aqueous HCl.

Data Availability Statement

The NMR spectra associated with this work are provided in the Supplementary Material accompanying this paper while the corresponding X-ray datasets (cifs) have been deposited with the Cambridge Crystallographic Data Centre (CCDC) and can be accessed as detailed under the section Structure Determinations.

Conflicts of Interest

The authors declare no conflicts of interest.

Declaration of Funding

As noted in the Acknowledgements section, funding for this work was provided by the Australian Government and Circa Group Ltd for providing an Innovations Connections grant and the Australian Research Council for providing a Laureate Fellowship to MLC.

Acknowledgements

We thank the Australian Government and Circa Group Ltd for the provision of an Innovations Connections grant. XL gratefully acknowledges Circa Group Ltd for providing a PhD stipend. Funding from the Australian Research Council (FL170100041) and supercomputing time on the National Facility of the Australian National Computational Infrastructure is also acknowledged. Circa Group Pty Ltd is thanked for providing access, through their license, to the software used for the reported COSMO-RS calculations and also for providing generous samples of LGO and Cyrene® used in this study.

References and Footnotes

1. (a) Gu, Y. L.; Jerome F. *Chem. Soc. Rev*. **2013**, *42*, 9550-9570; (b) Clarke, C. J.; Tu, W.-C.; Levers, O.; Bröhl, A.; Hallett, J. P. *Chem. Rev*. **2018**, *118*, 747-800; (c) Jordan, A.; Hall, C. G. J.; Thorp, L. R.; Sneddon, H. F. *Chem. Rev*. https://doi.org/10.1021/acs.chemrev.1c00672.
2. Sherwood, J.; De bruyn, M.; Contantinou, A.; Moity, L.; McElroy, C. R.; Farmer, T. J.; Duncan, T.; Raverty, W.; Hunt, A. J.; Clark, J. H. *Chem. Commun*, **2014**, *50*, 9650-9652.
3. (a) Pacheco, A. A. C.; Sherwood, J.; Zhenova, A.; McElroy, C. R.; Hunt, A. J.; Parket, H. L.; Farmer, T. J.; Constantinou, A.; De bryun, M.; Whitwood, A. C.; Raverty, W.; Clark, J. H. *ChemSusChem*. **2016**, *9*, 3503-3512. Also, see: (b) Milescu, R. A.; Zhenova, A.; Vastano, M.;Gammons, R.; Lin, S.; Lau, C. H.; Clark, J. H.; McElroy, C. R.; Pellis, A. *ChemSusChem.* **2021**, *14*, 3367-3381.
4. Camp, J. E. *ChemSusChem*, **2018**, *11*, 3048-3055.
5. See https://www.circagroup.com.au/cyrene (accessed 26/02/2022).
6. (a) Zhang, J.; White, G. B.; Ryan, M. D.; Hunt, A. J.; Katz, M. J. *ACS Sustainable Chem. Eng*. **2016**, *4*, 7186-7192; (b) Camp, J. E.; Nyamini, S. B.; Scott, F. J. *RSC Med. Chem*. **2020**, *11*, 111-117; (c) https://echa.europa.eu/registration-dossier/-/registered-dossier/16252 (accessed 26/02/2022).
7. Ma, X.; Anderson, N.; White, L. V.; Bae, S.; Raverty, W.; Willis, A. C.; Banwell, M. G. *Aust. J. Chem.* **2015**, *68*, 593-599.
8. (a) Ma, X.; Liu, X.; Yates, P.; Rafferty, W.; Banwell, M. G.; Ma, C.; Willis, A. C.; Carr, P. D. *Tetrahedron* **2018**, *74*, 5000-5011; (b) Diot-Néant, F.; Mouterde, L. M. M.; Couvreur, J.; Brunois, F.; Miller, S. A.; Allais, F. *Eur. Polym. J*. **2021**, *159*, 110745.
9. (a) Pecka, J.; Stanek, J.; Cerny, M. *Coll. Czech. Chem. Commun*. **1974**, *39*, 1192-1209; (b) Ton-That, T. *Nucleosides Nucleotides*, **1999**, *18*, 731-732.
10. Ledingham, E. T.; Greatrex, B. W. *Tetrahedron*, **2018**, *74*, 6107-6115.
11. Klepp, J.; Sumby, C. J.; Greatrex, B. W. *Synlett*. **2018**, *29*, 1441-1446.
12. (a) De bruyn, M.; Budarin, V. L.; Misefari, A.; Shimizu, S.; Fish, H.; Crockett, M.; Hunt, A. J.; Hofstetter, H.; Weckhuysen, B. M.; Clark, J. H.; Macquarie D. J. *ACS Sustainable Chem. Eng*. **2019**, *7*, 7878-7883; (b) Bousfield, T. W.; Pearce, K. P. R.; Nyamini, S. B.; Angelis-Dimakis, A.;, J. E. *Green Chem*. **2019**, *21*, 3675-3681.
13. (a) Rennecke, R.-W.; Eberstein, K.; Köll, P. *Chem. Ber*. **1975**, *108*, 3652-3655; (b) Shafizadeh, F.; Furneaux, R. H.; Stevenson, T. T. *Carbohydr. Res*. **1979**, *71*, 169-191.
14. Mouterde, L. M. M.; Allais, F.; Stewart, J. D. *Green Chem*. **2018**, *20*, 5528-5532.

15. (a) Shafizadeh, F.; Furneaux, R. H.; Pang, D.; Stevenson, T. T. *Carbohydr. Res*. **1982**, *100*, 303-313; (b) Kawai, T.; Isobe, M.; Peters, S. C. *Aust. J. Chem*. **1995**, *48*, 115-131; (c) Samet, A. V.; Niyazymbetov, M. E.; Semenov, V. V.; Laikhter, A. L.; Evans, D. H. *J. Org. Chem*. **1996**, *61*, 8786-8791; (d) Sharipov, B. T.; Pilipenko, A. N.; Valeev, F. A. *Russ. J. Org. Chem*. **2014**, *50*, 1628-1635; (e) Diot-Néant, F.; Mouterde, L.; Fadlallah, S.; Miller, S. A.; Allais, F. *ChemSusChem*. **2020**, *13*, 2613-2620.
16. Jeon, S.; Han, S. *J. Am. Chem. Soc*. **2017**, *139*, 6302-6305 and references cited therein.
17. Mancuso, A. J.; Swern, D. *Synthesis*, **1981**, 165-185.
18. For examples of the reactions of episulfonium ions with nitrogen-centred nucleophiles see Fox, D. J.; Morley, T. J.; Taylor, S.; Warren, S. *Org. Biomol. Chem*. **2005**, *3*, 1369-1371.
19. Horton, D.; Roski, J. P.; Norris, P. *J. Org. Chem*. **1996**, *61*, 3783-3793.
20. A single-crystal X-ray analysis of compound **12** has been reported previously although this did not establish, in contrast to the one reported here, its absolute configuration: Mamat, C.; Peppel, T.; Köckerling, M. *Crystals*, **2012**, *2*, 105-109.
21. Cantacuzene, J.; Petrissane, J.; Dang-Quoc-Quan. *Tetrahedron Lett*. **1967**, 2543-2545.
22. Hughes, L.; McElroy, C. R.; Whitwood, A.C.; Hunt, A. J. *Green Chem*. **2018**, *20*, 4423-4427 and references cited therein.
23. (a) Klamt, A.; Jonas, V.; Bürger, T.; Lohrenz, J. C. W. *J. Phys. Chem. A* **1998**, *102*, 5074-5085; (b) Klamt, A. *Wiley Interdiscip. Rev.: Comput. Mol. Sci.* **2018**, *8*, e1338.
24. Trasande, L. *The Lancet Planetary Health*, **2017**, *1*, e88-e89 and references cited therein.
25. Piersma, A. H.; Bosgra, S.; van Duursen, M. B. M.; Hermsen, S. A. B.; Jonker, L. R. A.; Kroese, E. D.; van der Linden, S. C.; Man, H.; Roelofs, M. J. E.; Schulpen, S. H. W.; Schwarz, M.; Uibel, F.; van Vugt-Lussenburg, B. M. A.; Westerhout, J.; Wolterbeek, A. P. M.; van der Burg, B. *Reproductive Toxicology*, **2013**, *38*, 53-64.
26. Schenk, B.; Weimer, M.; Bremer, S.; van der Burg, B.; Cortvrindt, R.; Freyberger, A.; Lazzari, G.; Pellizzer, C.; Piersma, A.; Schäfer, W. R.; Seiler, A.; Witters, H.; Schwarz, M. *Reproductive Toxicology*, **2010**, *30*, 200-218.
27. van der Burg, B.; Pieterse, B.; Buist, H.; Lewin, G.; van der Linden, S. C.; Man, H.-y.; Rorije, E.; Piersma, A. H.; Mangelsdorf, I.; Wolterbeek, A. P. M.; Kroese, E. D.; van Vugt-Lussenburg, B. *Reproductive Toxicology*, **2015**, *55*, 95-103.
28. A Panel of Quantitative Calux® Reporter Gene Assays for Reliable High-Throughput Toxicity Screening of Chemicals and Complex Mixtures in *High-Throughput Screening Methods in Toxicity Testing*, ed. Steinberg, P.; John Wiley & Sons (Hoboken, New Jersey, USA), 2013, pp 519-532.

29. van der Burg, B.; Wedebye, E. B.; Dietrich, D. R.; Jaworska, J.; Mangelsdorf, I.; Paune, E.; Schwarz, M.; Piersma, A. H.; Kroese, E. D. *Reproductive Toxicology*, **2015**, *55*, 114-123.
30. Krebs, A. et al. ALTEX, **2019**, *36*, 682-699.
31. Krebs, A., et al., *Arch. Toxicol*, **2020**, *94*, 2435-2461.
32. Byrne, F. P.; Nussbaumer, C. M.; Savin, E. J.; Milescu, R. A.; McElroy, C. R.; Clark, J. H.; van Vugt-Lussenburg, B. M. A.; van der Burg, B.; Meima, M. Y.; Buist, H. E.; Kroese, E. D.; Hunt, A. J.; Farmer, T. J. *ChemSusChem*, **2020**, *13*, 3212-3221.
33. van Vugt-Lussenburg, B. M. A.; van Es, D. S.; Naderman, M.; le Notre, J.; Klis, F. v. d.; Brouwer, A.; van der Burg, B. *Green Chemistry*, **2020**, *22*, 1873-1883.
34. Brattoli, M.; Cisternino, E.; Dambruoso, P. R.; de Gennaro, G.; Giungato, P.; Mazzone, A.; Palmisiani, J.; Tutino, M. *Sensors*, **2013**, *13*, 16759-16800.
35. Banwell, M. G.; Pollard, B.; Liu, X.; Connal, L. A. *Chem. Asian J*. **2021**, *16*, 604-620.
36. Still, W. C.; Kahn, M.; Mitra, A. *J. Org. Chem*., **1978**, *43*, 2923–2925.
37. Pangborn, A. B.; Giardello, M. A.; Grubbs, R. H.; Rosen, R. K.; Timmers, F. J. *Organometallics,* **1996**, *15*, 1518–1520.
38. Tozuka, H.; Ota, M.; Kofujita, H.; Takahashi, K. Synthesis of dihydroxyphenacyl glycosides for biological and medicinal study: β-oxoacetoside from *Paulownia tomentosa*. *J. Wood Sci*. **2005**, *51*, 48-59.
39. (a) Nagy, A.; Csordás, B.; Zsoldos-Mády, V.; Pintér, I.; Farkas, V.; Perczel, A. C-3 Epimers of sugar amino acids as foldamer building blocks: improved synthesis, useful derivatives, coupling strategies. *Amino Acids*, **2017**, *49*, 223-240; (b) Redlich, H.; Meyer, W.-U. *p*-Toluosulfinimidazolid als Reagenz zur haloenidfreien Sulfinesterbildung. *Liebigs Ann. Chem*., **1981**, 1354-1360.
40. Norris, P.; Fluxe, A. Preparation of a D-Glucose-Derived Alkene. *J. Chem. Ed*. **2011**, *78*, 1676-1678.
41. Dolomanov, O. V.; Bourhis, L. J.; Gildea, R. J.; Howard, J. A. K.; Puschmann, H. OLEX2: a complete structure solution, refinement and analysis program. *J. Appl. Cryst.* **2009**, *42*, 339-341.
42. Sheldrick, G. M. ShelXT-Integrated space-group and crystal-structure determination. *Acta Cryst*. **2015**, *A71*, 3-8
43. Sheldrick, G. M. Crystal structure refinement with *SHELXL*. *Acta Cryst*. **2015**, *C71*, 3-8.

44. Frisch, M. J.; Trucks, G. W.; Schlegel, H. B.; Scuseria, G. E.; Robb, M. A.; Cheeseman, J. R.; Scalmani, G.; Barone, V.; Petersson, G. A.; Nakatsuji, H., et al. *Gaussian 16 Rev. C.01*, Wallingford, CT, 2016.
45. Lu, T.; Chen, F., Multiwfn: a multifunctional wavefunction analyzer. *J. Comput. Chem.* **2012,** *33*, 580-592.
46. GaussView, Version 6, Dennington, Roy; Keith, Todd A.; Millam, John M. Semichem Inc., Shawnee Mission, KS, 2016.
47. http://cidportal.jrc.ec.europa.eu/ftp/jrc-opendata/EURLECVAM/datasets/DBALM/-LATEST/online/dbalm.html (accessed 29/06/2021).